Design of a Costas Loop to Operate With the Block III Receiver and Its Predicted Performance

G. Stevens and K. T. Woo
Communications Systems Research Section

A Costas loop has been designed and constructed to operate with the Block III receiver. It is a scaled-down version of the carrier tracking loop design in the Multimegabit Telemetry Demodulator and Detector (MTDD) unit under development. The constructed loop has been tested with the Block III Receiver at the Telecommunications Development Laboratory (TDL). This article describes its system design, hardware construction, and predicted performance.

I. Introduction

In order to test the compatibility of the current radiometric system in a DSN environment with suppressed carrier binary phase-shift keyed (BPSK) signalling and Costas loop carrier recovery, a Costas loop has been designed and constructed to operate with the Block III receiver. It has been tested with the Block III receiver at the Telecommunications Development Laboratory (TDL) and its measured performance, with respect to Doppler tracking, has been reported in Ref. 1. This article describes its design considerations. Its expected performance regarding steady state phase error under assumed Doppler conditions, rms phase jitter, and their respective sensitivities with respect to variations in signal-to-noise ratios are discussed. The loop's expected pull-in time is also given. System design considerations will first be discussed in Section II. Descriptions of hardware design and construction will be given in Section III. Predicted performance will be discussed in Sections IV, V, and VI.

II. System Design Considerations

The Costas loop is designed to be operated with the Block III Receiver in the long loop mode, controlling the VCO input, the output of which is multiplied to S-band for use in the first mixer. The system configuration is illustrated in Fig. 1. This loop will provide the Block III receiver with the option of tracking suppressed carrier signals, in addition to the existing capability of tracking residual carrier signals. In order to carry out the desired tests, as mentioned in Ref. 1, at the earliest time possible, the Costas loop modification is a scaled down version of the carrier tracking loop to be used in the Multimegabit Telemetry Demodulator and Detector (MTDD) now under development. In particular, this current Costas loop design utilizes a complex mixer which was developed in earlier projects (Refs. 2 and 3) and has a bandwidth of less than 2 MHz. Because of this inherent bandwidth limitation the designed Costas loop can only track signals having data rates up to 1 megasymbol per second (MSPS).

The Costas loop constructed has a hard limited inphase channel, so that the third multiplier which derives the loop error signal is a chopper-type device. This is illustrated in Fig. 2. The inphase (I) and quadrature (Q) arm filters are one-pole RC filters, which are scaled to the data rates received. The loop filter has transfer function of the form

$$F(s) = \frac{1 + \tau_2 s}{1 + \tau_1 s} \tag{1}$$

so that the loop is a second order loop.

The design goal of this loop is to be able to track suppressed carrier BPSK signals with symbol SNR's (ST/N_o) as low as −4 dB with an rms phase jitter less than or equal to 3 degrees. In addition, the steady state phase error is to be less than or equal to 3 degrees with Doppler offsets less than 2 kHz and Doppler rates of 2 Hz/s or less. The design parameters to be determined in a Costas loop are the arm filter bandwidths and the loop filter time constants, or equivalently, the squaring losses (Ref. 4), loop bandwidths (B_L) and damping factor (ξ), in addition to the open loop gain. In order to meet the steady state phase error requirements it is shown in Section V that the total loop gain has to satisfy

$$K_T \geq 2.4 \times 10^5 \tag{2}$$

The loop bandwidth constraint, in order to meet the jitter requirement, is found to be

$$B_L T \leq 2.4 \times 10^{-4} \tag{3}$$

where $1/T$ is the data rate received. For the four data rates of concern in Ref. 1, the loop bandwidths are, at the design point with ST/N_O = −4 dB, selected from Table 1. These loop bandwidths are design point values and they increase with ST/N_O. The arm filter noise bandwidths are chosen to equal twice the data rate, so that squaring losses are acceptable.

With the desired damping factor set to be $\xi = 0.707$ at design point values, and with the loop gain K_T satisfying Eq. (2), and B_L's given in Table 1, the time constants τ_1, τ_2 in the loop filter can be determined. They are given in Table 2.

Further discussions on performance evaluations are given in Sections IV, V, and VI. In the next section we first describe the hardware design of the Costas loop.

III. Description of Hardware Design

A block diagram of the Costas loop phase detector and loop filter assembly hardware is shown in Fig. 3. The 10 MHz IF signal is amplified and applied to the input of a 2-way power splitter. One output drives a true rms voltmeter which is used as a signal level monitor when adjusting the IF signal level. The other power splitter output drives a 10 MHz quadrature IF mixer (complex mixer). Inphase and quadrature (I&Q) baseband signals are generated by the complex mixer by splitting the IF signal into two paths and mixing with 10 MHz LO signals which are in phase quadrature. The resulting baseband mixer products are then bandlimited to 2 MHz by 2-section elliptic low pass filters. A detailed description of the complex mixer is given in Refs. 2 and 3.

The inphase and quadrature baseband signals generated by the complex mixer are next passed through identical arm filters. Simple resistance-capacitance (RC) low pass filters are used when processing signals in which the carrier is biphase modulated directly by the data symbols. When the data is modulated onto a square wave subcarrier, the low pass arm filters are replaced by resistance-inductance-capacitance (RLC) bandpass filters, whose passbands are centered at the subcarrier fundamental frequency. Inphase and quadrature baseband signals generated by the complex mixer are also buffered and supplied to test points to facilitate wave form inspection with an oscilloscope.

A hard limiter follows the inphase channel's arm filter. The output of the quadrature channel's arm filter is linearly amplified. These two signals are then multiplied together in a double balanced mixer whose output drives an active lead/lag loop filter. The loop filter's output is supplied to the receiver's voltage-controlled crystal oscillator in its LO chain. Variable gain control and an inverted output are provided in the loop filter and amplifier. A built-in voltmeter monitors the VCO control voltage. Offset currents generated within the Costas loop's phase detector are cancelled by an offset adjustment potentiometer.

In this Costas loop design the bandwidths of the RC-arm filters are chosen to be twice the received data rate. The arm filter design is illustrated in Fig. 4, while the respective parametric values of the filter components are described in Table 3.

The loop filter design, corresponding to the time constants described in Table 2, is illustrated in Fig. 5, with its component values given in Table 4.

IV. Tracking Analysis of the Costas Loop

The tracking performance of a Costas loop with hard limited in phase channel has been analyzed in detail in Ref. 4. Basically, the steady state phase error and the rms phase jitter of the loop are dependent upon the signal suppression factor $\tilde{\alpha}$ and the squaring loss factor S_L, in addition to other design parameters such as loop filter time constants and the gains of the phase detector and the VCO.

Signal suppression on the loop error signal is due to the arm filters and the hard limiter, and varies with ST/N_o and the choice of arm filter bandwidth relative to the data rate. When the arm filters are one-pole RC filters, this signal suppression factor $\tilde{\alpha}$ has been evaluated in Ref. 4. The results are shown here in Fig. 6. The total loop gain in the Costas loop design as described in Section III is dependent upon $\tilde{\alpha}$ through the following relationship:

$$K_T = \tilde{\alpha}\sqrt{S}\ K_p K_v K_{LF} \tag{4}$$

where S is the average signal power at the output of the manual gain control (MGC) unit, K_p is the phase detector gain, K_v is the VCO gain, and K_{LF} is the variable loop filter gain as described in Section III. Both loop bandwidth and damping varies with loop gain, and they are thus also SNR dependent. The same is thus also true for the steady state phase error and the rms phase jitter of the loop. These dependences are further discussed in Section V.

The rms phase jitter of the loop for a given loop bandwidth B_L is given by Ref. 4.

$$\sigma_\phi^2 = \left[\left(\frac{ST}{N_o}\right)\left(\frac{1}{B_L T}\right) S_L\right]^{-1} \tag{5}$$

where S_L is the squaring loss factor, which is less than unity, and is also dependent upon ST/N_o and the arm filter bandwidth. The squaring loss of the Costas loop with a hard limited in phase channel and one pole low pass RC arm filters has been evaluated in Ref. 4, and the results are included in Fig. 7 for reference.

With $\tilde{\alpha}$ and S_L known from Figs. 6 and 7 it is then straight forward to determine the parameters in the loop design and to predict the performance of loop as ST/N_o varies. These are discussed in the next section.

V. Determination of Design Parameters and Performance Predictions

The basic parameters to be determined in the loop design are: the arm filter bandwidth, the total loop gain K_T, and the time constants τ_1 and τ_2 in the loop filter. The values of K_T, τ_1 and τ_2 also determine the loop bandwidth B_L and the damping factor ζ.

The selection of arm filter bandwidth affects the squaring loss S_L of the Costas loop, as illustrated in Fig. 7. It is observed from Fig. 7 that S_L varies from -5 to -9 dB for choices of arm filter bandwidths from 0.75 to 4.5 times the data rate, at the design point ST/N_o of -4 dB. Even though not shown on Fig. 7, the squaring loss S_L decreases rapidly when the arm filter bandwidth decreases below $0.75/T$, where $1/T$ is the symbol rate. Squaring loss is least when the arm filter bandwidth B is around $1/T$. And as B increases above $1/T$, S_L decreases monotonically again. Nevertheless, S_L is relatively constant for BT values ranging from 0.75 to 2.5. In this particular design the one pole RC arm filters are chosen to have a BT product of 2. The squaring losses with the arm filter bandwidth selected in this way will be less than 0.6 dB for all $ST/N_o > -4$ dB.

With a squaring loss of 6.6 dB or less the required loop bandwidth B_L at the design point ST/N_o of -4 dB can be chosen, in order to have rms phase jitter below 3 degrees, according to Eq. (5) as follows:

$$B_L T \leq \left(\frac{ST}{N_o} S_L\right)\left(\frac{\pi}{60}\right)^2 = 2.4 \times 10^{-4} \tag{6}$$

This resulted in the design point loop bandwidths listed in Table 1.

Next we consider the total open loop gain K_T. The steady state phase errors due to a radian Doppler offset Ω_0 and a Doppler rate Ω_1 are Ω_0/K_T and Ω_1/ω_n^2 respectively, for a second order loop (Ref. 5), where ω_n is the natural frequency of the loop. Assuming we choose a damping factor of ζ of 0.707 at the design point, the values of ω_n for the selections of B_L shown in Table 1 will be ≥ 45. The steady state phase error due to a Ω_1 of 2 Hz/s will then be ≤ 0.35 degrees. The combined steady state phase error ϕ_{ss} due to both Ω_0 and Ω_1 can be modeled as

$$\phi_{ss} = \sqrt{\left(\frac{\Omega_0}{K_T}\right)^2 + \left(\frac{\Omega_1}{\omega_n^2}\right)^2} \tag{7}$$

In order for ϕ_{ss} to be ≤ 3 degrees for a Doppler offset of 2 kHz and a Doppler rate of 2 Hz/s it follows from Eq. (7) that the total loop gain K_T must satisfy

$$K_T \geq \frac{\Omega_0}{\sqrt{\phi_{ss}^2 - (\Omega_1/\omega_n^2)^2}} \geq 2.4 \times 10^5 \qquad (8)$$

With K_T determined as above it is straightforward to determine the variable loop filter gain K_{LF} from Eq. (4), given the signal power S, the VCO gain K_v, and the phase detector gain K_p. The VCO gain K_v in block III is equal to $2\pi \times 96 \times 400$ radians/volt. The phase detector gain K_p is measured to be 0.646 volts/radians. However, the signal level $\sqrt{S}$ is SNR dependent, since it is controlled by a manual gain control (MGC) which holds the signal plus noise power constant in the IF bandwidth (B_{IF}) of 7.92 MHz. It can be derived that the signal level $\sqrt{2S}$ after MGC is given by

$$\sqrt{2S} = \frac{\sqrt{2}\,\lambda}{\sqrt{1 + \dfrac{B_{IF}T}{(ST/N_o)}}} \qquad (9)$$

where $\lambda = 0.15$ volt is the desired average signal plus noise power in the MGC output and is determined by the appropriate input level to the complex mixer as described in Section II. Since $\tilde{\alpha}$ equals 0.298 at $ST/N_o = -4$ dB with arm filter $BT = 2$, the loop filter gain K_{LF} is then determined from Eqs. (4), (8), and (9) to be:

$$K_{LF} = \frac{K_T}{\tilde{\alpha} K_p K_v \sqrt{S}} = \frac{2.4 \times 10^5}{(0.298)(0.646)(2\pi \times 96 \times 400)\dfrac{\sqrt{2} \times 0.15}{\sqrt{1 + \dfrac{B_{IF}T}{ST/N_o}}}} \qquad (10)$$

At the design point $ST/N_o = -4$ dB, with $B_{IF} = 7.29$ MHz, these required values of K_{LF}'s are determined to be the following:

Variable Loop Filter Gain Settings K_{LF}

Data Rates	K_{LF}
100 KSPS	331
250	210.5
500	149.6
1000	107

With B_L requirements given in Table 1 and total open loop gain K_T requirements given in Eq. (7), it is straightforward to determine the loop filter time constants τ_1 and τ_2 from the following well-known relationships (Ref. 5) of second order loops with loop filters of the forms given in Eq. (1):

$$\tau_1 = \frac{K_T}{\omega_n^2} \qquad (11)$$

$$\tau_2 = \frac{2\omega_n \tau_1 \zeta - 1}{K_T} \qquad (12)$$

Requiring ζ_o (design point value) to be 0.707, so that $\omega_n = 1.89\,B_L$, the respective values of τ_1 and τ_2 are determined from Eqs. (11) and (12) to be those given in Table 2.

Next we consider the performance of this loop design as ST/N_o increases above -4 dB. Both $\tilde{\alpha}$, K_T, S_L and B_L are dependent upon ST/N_o. The dependences on ST/N_o of $\tilde{\alpha}$ and S_L have already been given in Figs. 6 and 7. The dependence of K_T on ST/N_o comes from $\tilde{\alpha}$ as well as the signal $\sqrt{S}$ level after MGC, as given in Eq. (10). From K_T and τ_1 the natural frequency ω_n of the loop can be determined from Eq. (11), and from which ζ can be determined from Eq. (12). Given ω_n and ζ, B_L can be determined by the following well known relationship (Ref. 5) of second order loops:

$$B_L = \frac{\omega_n}{2}\left(\zeta + \frac{1}{4\zeta}\right) \qquad (13)$$

The dependences of B_L and ζ on ST/N_o are plotted in Figs. 8 and 9 for this Costas loop design. Given B_L, S_L, the rms jitter can be determined from Eq. (5). Also, the steady state phase error, given K_T and ω_n, can be determined from Eq. (7). Their respective dependencies upon ST/N_o are plotted in Figs. 10 and 11.

VI. Pull-in Time Considerations

In the absence of noise, the dynamic loop error signal in Fig. 2 has the form

$$\epsilon(t) = K_p \operatorname{sgn}\left[\sqrt{S}\,\widehat{d(t)\cos\phi(t)}\right]\left[\sqrt{S}\,\widehat{d(t)\sin\phi(t)}\right] \qquad (14)$$

where $\phi(t)$ is the phase error process, $d(t)$ is the baseband data waveform, and the notation "$\widehat{\ }$" is used to denote the

operation of the arm filters. Suppose we assume the filtering operation is negligible, which will be seen to be justifiable for pull-in time considerations, then the differential equation that governs the dynamics of the Costas loop is given by

$$\frac{d\phi}{dt} = \frac{d\theta}{dt} - KF(p)\ \{\text{sgn}\ [\cos\phi(t)]\ \sin\phi(t)\} \quad (15)$$

where θ is the received carrier phase, F is the loop filter transfer function, p is the Heaviside operator d/dt, and K is a constant proportional to the signal level, the VCO gain, and the phase detector gain. Strictly speaking, K depends also upon the frequency offset between the local VCO and the incoming carrier. The function sgn $[\cos\phi(t)]$ can be expressed in a Fourier series:

$$\text{sgn}\ [\cos\phi(t)] = \frac{4}{\pi}\sum_{k=0}^{\infty}\frac{(-1)^k}{2k+1}\cos\ [(2k+1)\phi(t)] \quad (16)$$

which consists only of odd harmonics of $\phi(t)$. During the acquisition phase the term corresponding to $k = 0$ has the dominant effect on the loop, since all terms in Eq. (16) pass through the loop filter. Thus, to a good approximation, the behavior of the Costas loop, neglecting the arm filters and ignoring higher-order Doppler derivatives, is governed by:

$$\frac{d\tilde{\phi}}{dt} = \tilde{\Omega}_0 - 2K'F(p)\sin\tilde{\phi} \quad (17)$$

where $\tilde{\phi} = 2\phi$, $K' = (2/\pi)K$, and $\tilde{\Omega}_0 = 2\Omega_0$, where Ω_0 is the initial frequency offset in radians per second. The $\tilde{\phi}$ process then satisfies the same well-known differential equation (Ref. 5) that is satisfied by an ordinary phase lock loop. The effective Doppler offset is now $2\Omega_0$, and the effective gain is $2K'$.

During tracking $\tilde{\phi} \approx 0$ and Eq. (17) can be linearized to be

$$\frac{d\tilde{\phi}}{dt} = \tilde{\Omega}_0 - 2K'F(p)\tilde{\phi} \quad (18)$$

Let $\tilde{\zeta}$ and $\tilde{\omega}_n$ denote the damping factor and natural frequency, respectively, of the linearized model Eq. (18). Then $\tilde{\zeta}$ and $\tilde{\omega}_n$ are equal to $\sqrt{2}\,\zeta$ and $\sqrt{2}\,\omega_n$ respectively, where ζ and ω_n are those given in Eqs. (11) and (12) which correspond to the linearized differential equation governing ϕ rather than $\tilde{\phi}$. This is because the gain in Eq. (18) is $2K'$ rather than K'. The pull-in range of the Costas loop model (17) can then be given in the same way as that of a phase lock loop (Ref. 5):

$$|\tilde{\Omega}_0| = |2\Omega_0| \leq 2\sqrt{(2K')\tilde{\zeta}\tilde{\omega}_n}$$

$$= 4\sqrt{K'\zeta\omega_n} \quad (19)$$

This implies $|\Omega_0| \leq 2\sqrt{K'\zeta\omega_n}$. Suppose the initial frequency offset is small compared to the arm filter bandwidth; then K' here should be very close to K_T, the total loop gain design parameter discussed in Section V. For the design at 100 KSPS discussed in Section V with $K_T = 2.4 \times 10^5$, $\tau_1 = 112.5$ s, and $\tau_2 = 0.03124$ sec, ζ is 0.707 and ω_n is 46.2. When these values are substituted in Eq. (19), the pull-in range is computed to be

$$\left|\frac{\Omega_0}{2\pi}\right| < 894\ \text{Hz}$$

This pull-in range is much narrower than the arm filter bandwidth, which equals 200 kHz when the received data rate is 100 KSPS, so we are justified in neglecting arm filter effects for this computation.

The pull-in time of the loop model governed by Eq. (17) can now be computed in the same way as that of the phase lock loop (Ref. 5):

$$T_{acq} = \frac{\tilde{\Omega}_0^2}{2\tilde{\zeta}\tilde{\omega}_n^3} = \frac{(2\Omega_0)^2}{2\sqrt{2}\,\zeta(\sqrt{2}\,\omega_n)^3} = \frac{\Omega_0^2}{2\zeta\omega_n^3} \quad (20)$$

For the loop design at 100 KSPS mentioned previously the pull-in times for various initial frequency offsets are given in Table 5. These predictions agree closely with measurements reported in Ref. 1.

VII. Conclusions

The design and performance prediction of the Costas loop tested with the Block III receiver at TDL as reported in Ref. 1 is documented in this paper. The test results reported in Ref. 1 are found to be in good agreement with these performance predictions.

References

1. Reasoner, R., Stevens, G., and Woo, K. T., "Costas Loop Demodulation of Suppressed Carrier BPSK Signals in the DSN Environment – Experimental Results Obtained at TDL", this issue of *The DSN Progress Report*.

2. Constenla, L. C., "Complex Mixer System," Technical Report 32-1526, Jet Propulsion Laboratory, Pasadena, California, Dec. 15, 1972.

3. Stevens, G. L., "Complex Mixer System Modifications," *The DSN Progress Report 42-42*, Jet Propulsion Laboratory, Pasadena, California, Sept. and Oct., 1977, pp. 88-91.

4. Simon, M. K., "Tracking Performance of Costas Loops With Hard-Limited In-Phase Channel," *IEEE Trans. on Comm.*, Vol. COM-26, No. 4, Apr. 1978, pp. 420-432.

5. Viterbi, A., *Principles of Coherent Communications*, McGraw Hill Book Co., New York, NY, 1966.

Table 1. Loop bandwidths

Data rates	Design point Loop bandwidth at ST/N_o = -4 dB
100 KSPS	24.04 Hz
250 KSPS	60.1 Hz
500 KSPS	122.2 Hz
1000 KSPS	244.4 Hz

Table 2. Loop filters

Data rates	Loop filter time constants	
	τ_1	τ_2
100 KSPS	112.50 s	0.03124 s
250 KSPS	18.00 s	0.01246 s
500 KSPS	4.500 s	0.006117 s
1000 KSPS	1.125 s	0.00306 s

Table 3. Arm filter designs

Data rates	$2\pi \times f_c$	R	C
100 KSPS	8×10^5 rad/s	510 Ω	2451 pf
250 KSPS	2×10^6 rad/s	510 Ω	980 pf
500 KSPS	4×10^6 rad/s	510 Ω	490 pf
1000 KSPS	8×10^6 rad/s	510 Ω	245 pf

(f_c = 3 dB corner frequency)

Table 4. Loop filter designs

Data rates	R_1	R_2	R_3	C
100 KSPS	50K	3.08K	10M	9.92 μf
250 KSPS	50K	6.68K	10M	1.866 μf
500 KSPS	50K	13.6K	10M	0.4498 μf
1000 KSPS	50K	27.2K	10M	0.1125 μf

Table 5. Pull-in times of the Costas loop design receiving data rate at 100 KSPS

Initial frequency offset	Pull-in time
100 Hz	2.83 s
200 Hz	11.3 s
300 Hz	25.47 s
400 Hz	45.25 s

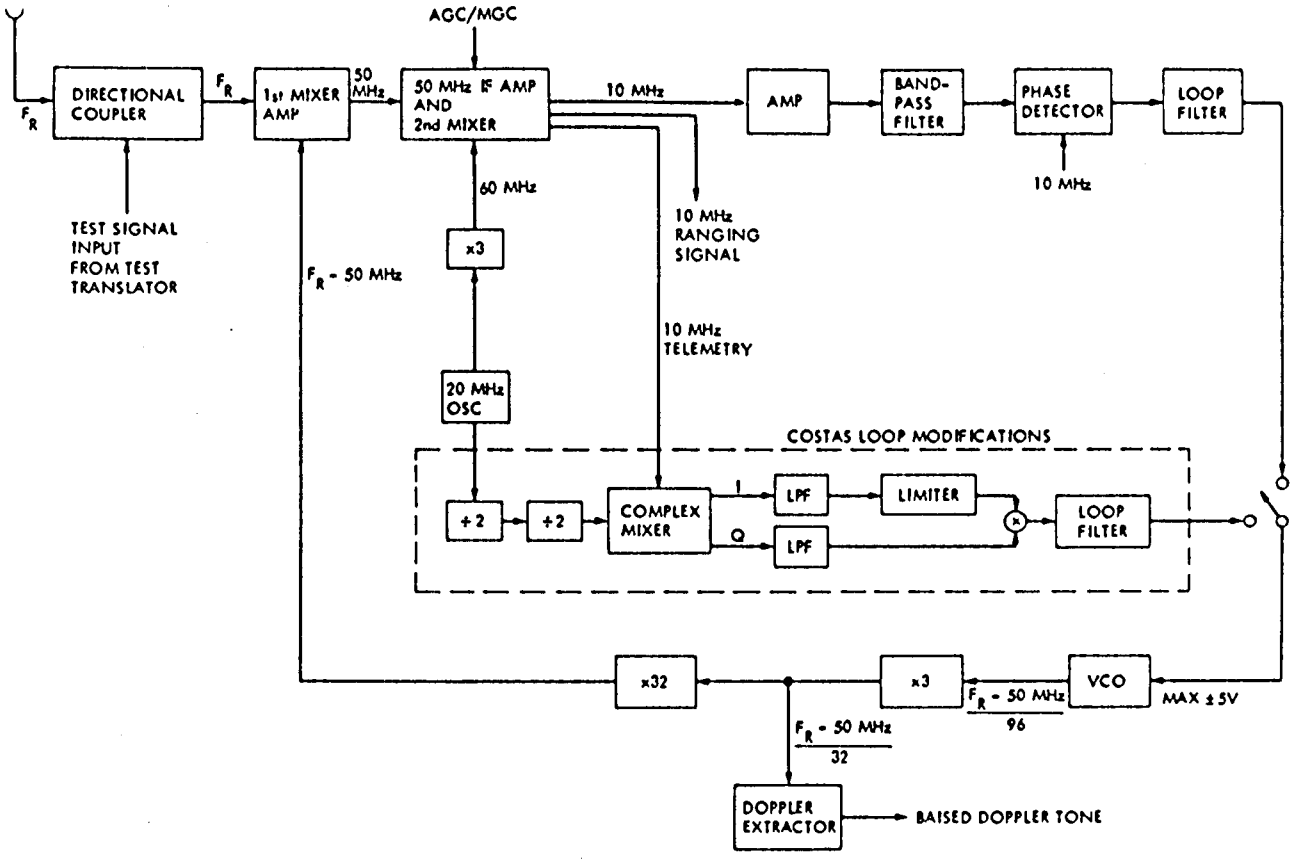

Fig. 1. Modification of block III receiver to include Costas loop

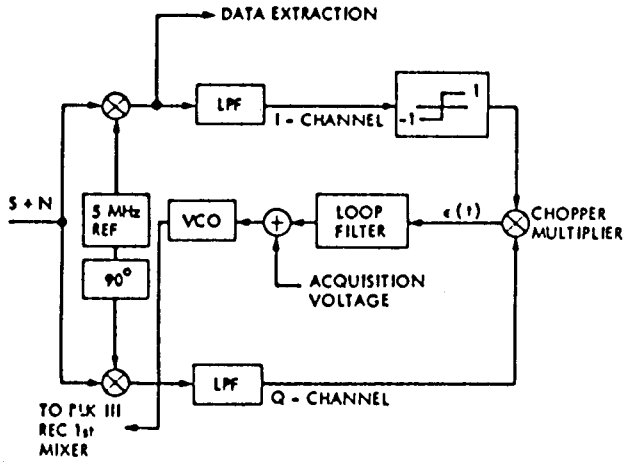

Fig. 2. Functional block diagram of a Costas loop with hard limited inphase channel

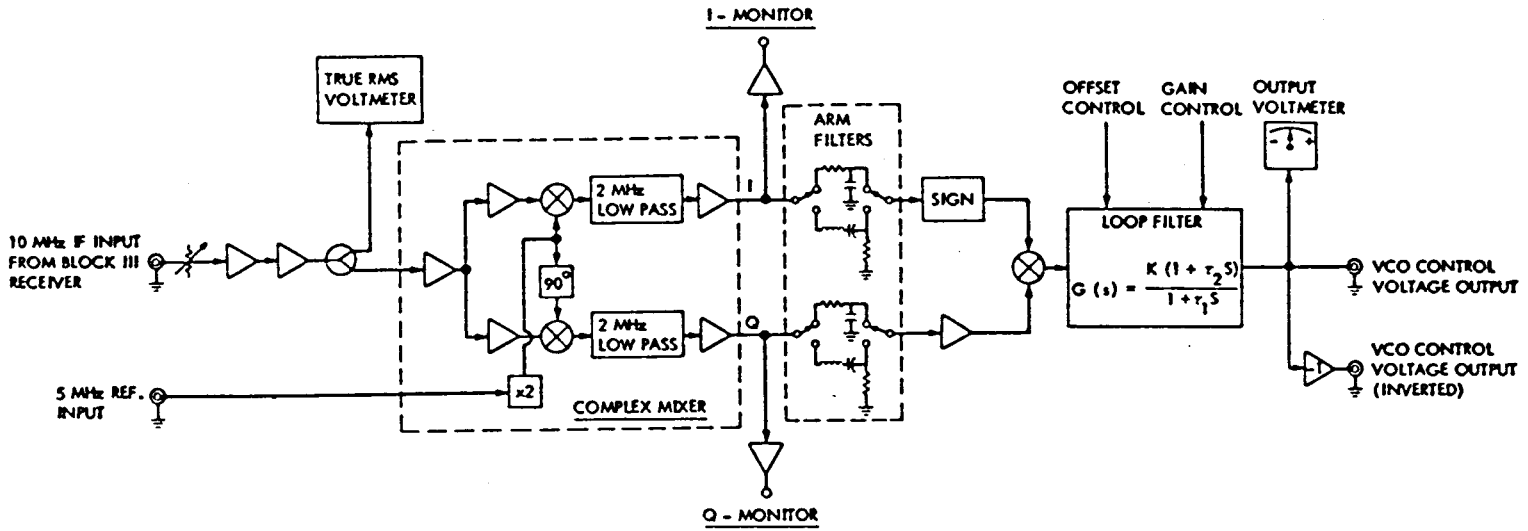

Fig. 3. Block diagram of analog Costas loop hardware

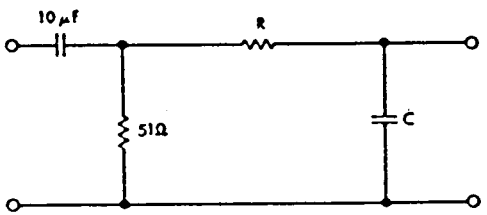

Fig. 4. Block diagram of A-C coupled low pass arm filters

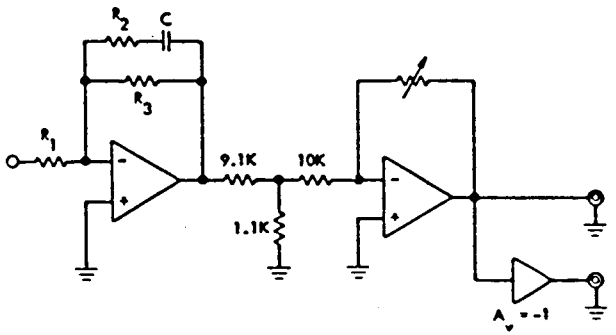

Fig. 5. Block diagram of loop filter design

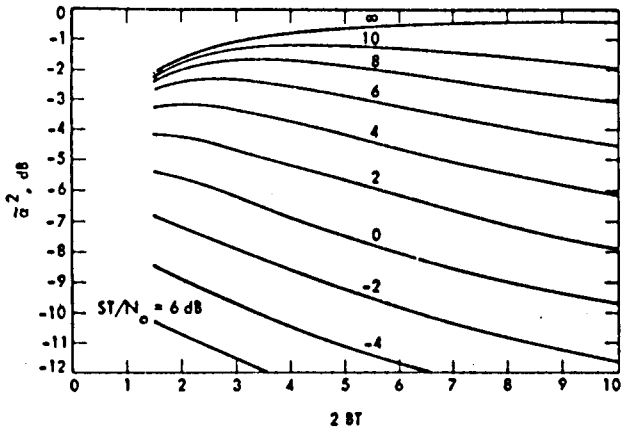

Fig. 6. Signal power suppression factor vs the ratio of two-sided arm filter bandwidth to data rate with signal-to-noise ratio as parameter.

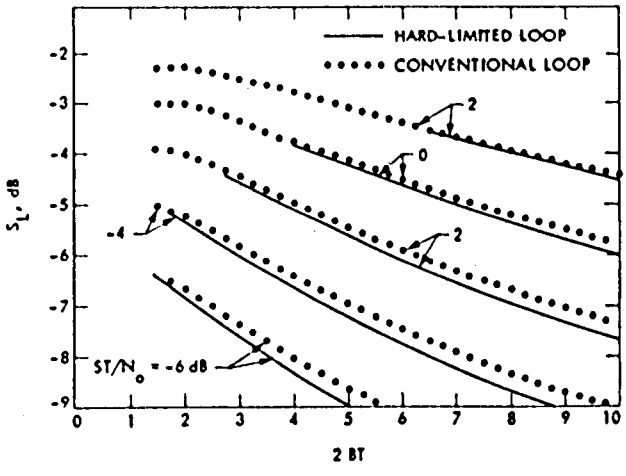

Fig. 7. Squaring loss variations vs $2BT$, with ST/N_0 as a parameter; small SNR approximation; RC filter, NRZ data.

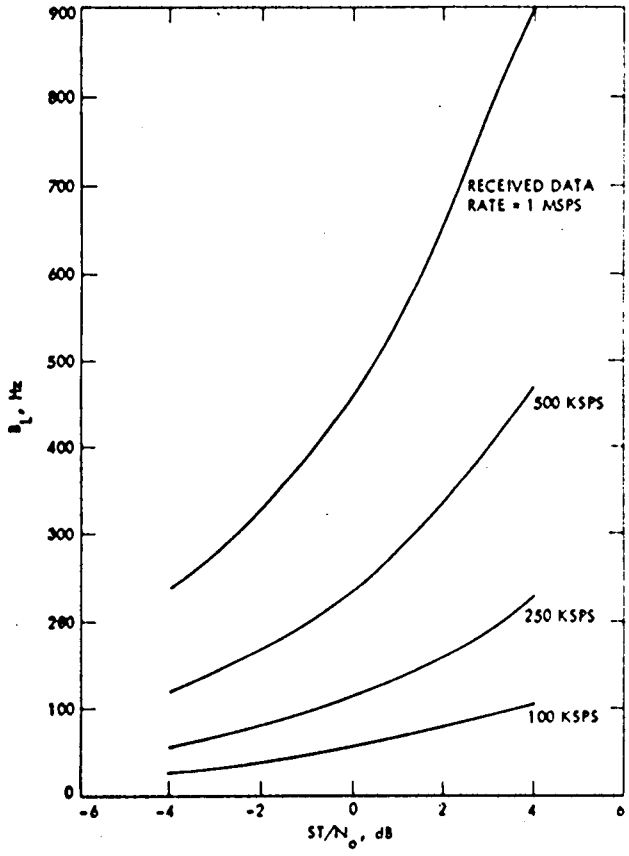

Fig. 8. Design values of Costas loop noise bandwidth as functions of ST/N_0

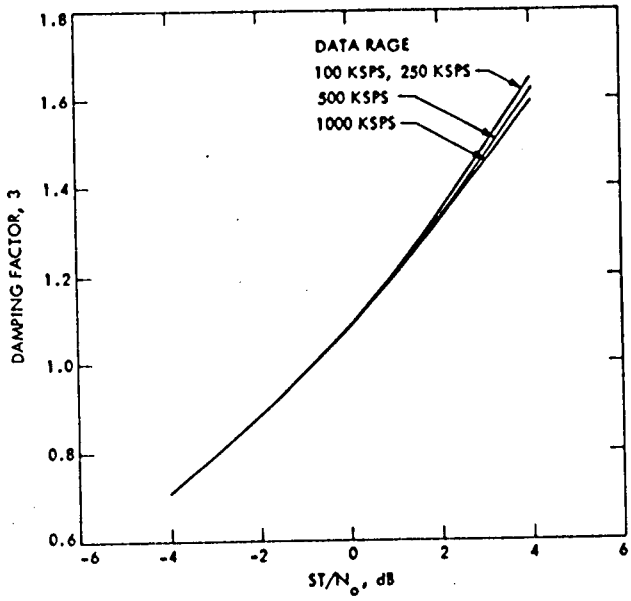

Fig. 9. Design values of Costas loop damping factor as functions of ST/N_0

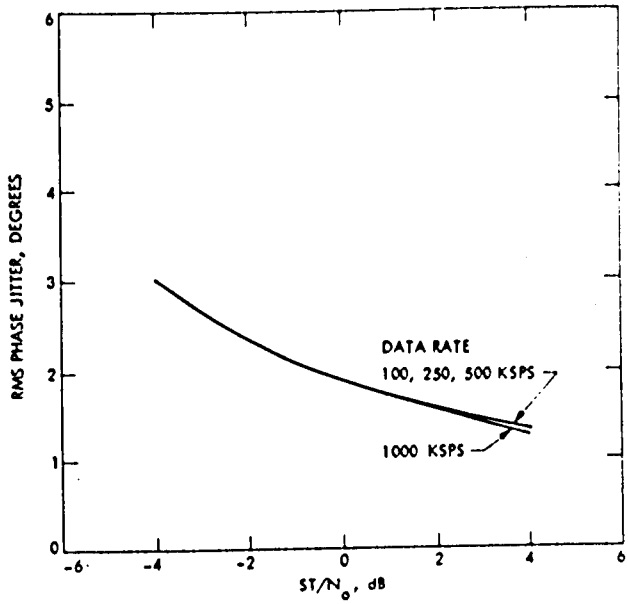

Fig. 10. Design values of Costas loop rms phase jitters as functions of ST/N_0

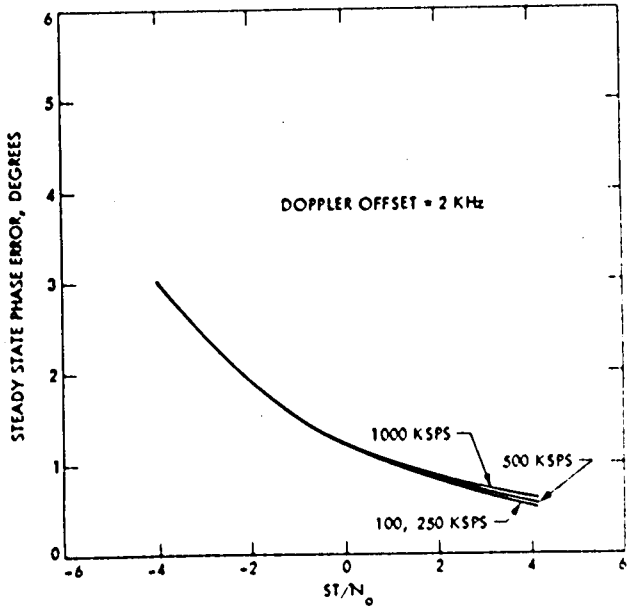

Fig. 11. Design values of Costas loop steady state phase errors as functions of ST/N_0